Chapter 1

Cluster Formation and Early Evolution

The formation and properties of stellar streams (their density and velocity structure, their size and shape, and their binary fraction) depend on the properties of their progenitors. In this section we will explore the formation and early evolution of globular clusters, including an approximate prescription for the mass-size relations of dense massive clusters, the effects of mass loss from stellar evolution and gas expulsion, and the initial binary population.

1.1 Early mass-size relations

Recommended reading: Fujii & Zwart 2016 ($\S 1, 5.1, 5.2$), Kamdar et al. 2019 ($\S 2.4.3$)

Star clusters are classically characterized as “open” and “globular.” Open clusters are younger (often but not always $\lesssim 1$ Gyr; exceptions include M67 N188, N6791) with of order 100–10^4 stars, and typically have disk-like orbits, whereas globular clusters are old ($\gtrsim 10$ Gyr), more massive and dense, and with halo-like orbits. While an exact boundary between the two is likely artificial, our interest here is in the denser clusters which evolve to form thin streams in the Galactic halo.

We cannot observe Milky Way globular clusters at their formation to measure their initial mass-size relations, but we can seek clues from a subset of open clusters known as “young massive clusters,” which have ages $\lesssim 10$ Myr and are extremely dense. YMCs are rare in the Milky Way, but common in nearby starburst galaxies. They form from the densest molecular clouds, where the star formation efficiency depends on the gas density, and their

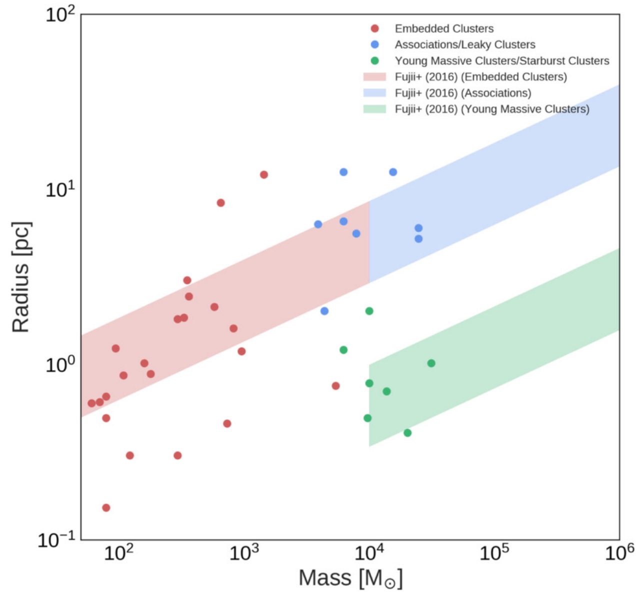

Figure 1.1: From Kamdar et al. (2019), summarized size-mass relations for embedded clusters, associations, and young massive clusters of age $t = 1$–5 Myr. Observational values are over-plotted.

evolution seems to follow a distinct track from that of classical open clusters (which evolve from embedded clusters and into unbound "associations"). This is illustrated in Figure 1.1, which shows mass-radius relations for young clusters ($1 < t_{\rm age} < 5$ Myr) compiled by Fujii & Zwart (2016), overlayed with observations of clusters in each category. Fujii & Zwart (2016) argue for a boundary between bound "clusters" and unbound "associations" where the cluster age equals the dynamical timescale (so that a group of stars with a density too low to be a bound cluster will have a dynamical timescale exceeds its age). This allows them to derive a scaling relation between cluster mass, radius and age:

$$t_{\rm age} \propto \frac{1}{\sqrt{\rho}}; \qquad\qquad \rho \propto \frac{M}{R^3}$$
$$\Rightarrow R \propto (M)^{1/3}(t_{\rm age})^{2/3}. \tag{1.1}$$

The separate track for YMCs shown by the shaded green region of Figure 1.1 can be understood as resulting from much higher initial densities compared to classical open clusters, while sharing the same power law dependence. See §5.2 of Fujii & Zwart (2016) for further theoretical detail.

There is a considerable amount of scatter among the observations in Figure 1.1, which Kamdar et al. (2019) attribute to the fact that different regions of the parameter space are sensitive to different feedback mechanisms, and that it is difficult to observationally define

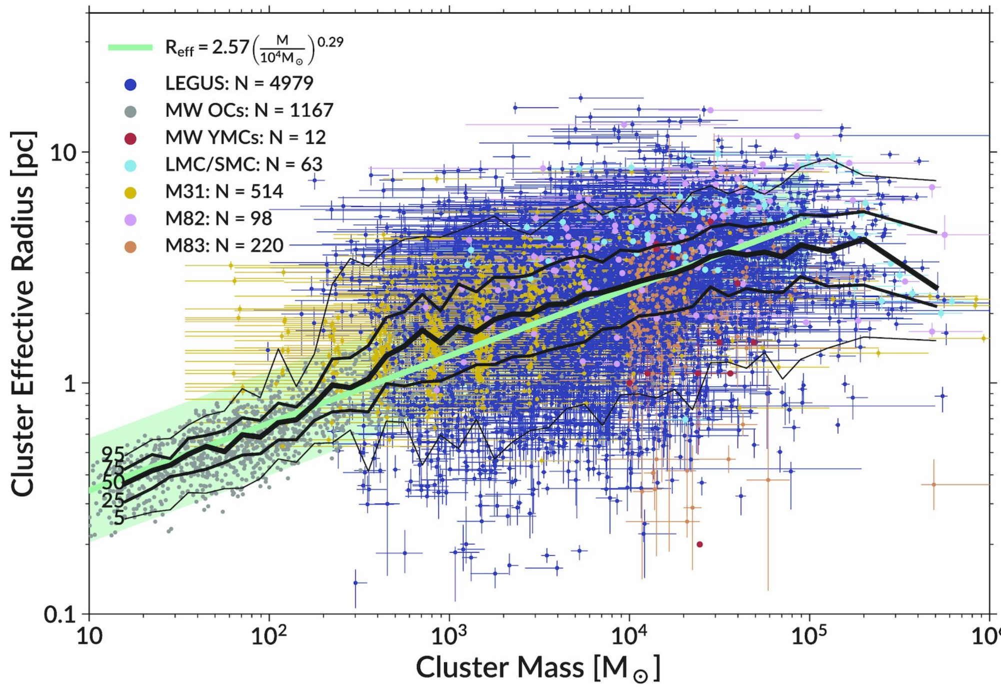

Figure 1.2: Figure 13 from Brown & Gnedin (2021), showing the masses and radii of young clusters (< 1 Gyr) in LEGUS as well as several other data sets. The mass-radius relation fit to these data is shown by the solid green line (whose equation is in the top left corner).

embedded clusters while they are still shrouded by a natal cloud.

Brown & Gnedin (2021) offer a larger dataset of YMCs in the Legacy Extragalactic UV Survey (LEGUS). Figure 1.2 shows their distribution in mass and radius (for clusters < 1 Gyr), along with several other datasets noted in the legend. They fit a power law with slope ~ 0.24, slightly shallower than that from Fujii & Zwart (2016). Excluding all but the youngest clusters, aged 1–10 Myr, Brown & Gnedin (2021) fit an even shallower slope of $\sim$0.18 (see their Table 2). In strongly lensed high-redshift galaxies, it is sometimes possible to fit the SEDs and measure the properties of "clumps" likely to be true globular cluster precursors. For example, Claeyssens et al. (2023) find a similar power law to that in Figure 1.2, but in clump populations in lensed galaxies imaged by JWST (see their §6.4).

The main takeaway here is that, while the exact physics governing their formation is not well understood, YMCs and presumably ancient globular clusters are/were extremely dense. A $10^4 M_\odot$ cluster with stellar masses following a Kroupa (2001) IMF contains 15–20000 stars, which begin their lives confined to region of order 1 pc in size.

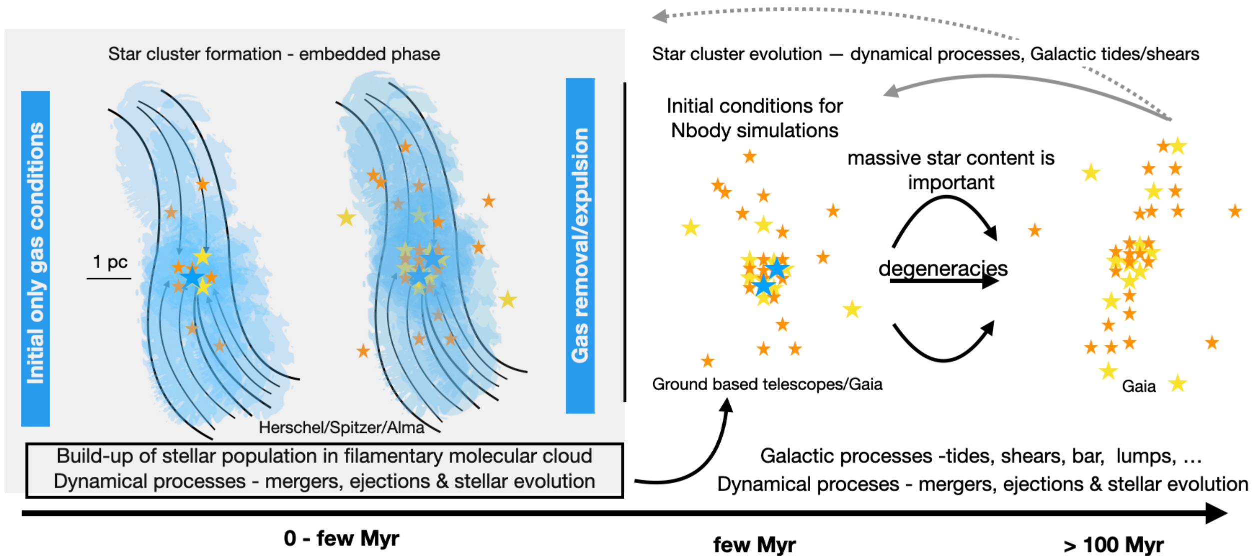

Figure 1.3: Figure 2 from Wang & Jerabkova (2021), sketching the formation and evolution of a star cluster.

1.2 Mass loss from stellar evolution

Recommended Reading: Hills (1980); Lada et al. (1984); Baumgardt & Kroupa (2007); Binney & Tremaine 2008 (§ 7.5.1)

Stars eject material from their surfaces throughout their lives (and of course the most massive stars end their short lives in supernovae). As material ejected by stars escapes cluster, it sweeps out any gas that has not formed stars, giving rise to cluster mass loss through gas expulsion on top of the material lost from the stars themselves. Figure 1.3 sketches the formation and early evolution of a star cluster, including gas removal, mass loss from stellar evolution, and the formation of tidal tails.

Below, we treat the issue of cluster mass loss analytically, following Hills (1980) and B&T §7.5.1.

At early times (on the left hand side of Figure 1.3), as the most massive stars in the cluster evolve, the mass loss is impulsive, occurring quickly compared to the cluster's dynamical/crossing timescale ($\tau_D = (G\rho)^{-1/2}$ for a cluster of density ρ). If we assume that a cluster of total mass M_0 and size R_0 consists of formed stars in dynamical equilibrium before mass loss, it obeys the virial theorem:

$$2K_0 + W_0 = 0, \tag{1.2}$$

where, for average stellar velocity $\langle v_0 \rangle$

$$K_0 = \frac{M_0 \langle v_0^2 \rangle}{2}; \quad W_0 = -\frac{GM_0^2}{2R_0}; \quad \Rightarrow \langle v_0^2 \rangle = \frac{GM_0}{2R_0}. \tag{1.3}$$

Note that using $E = K + W$, the virial theorem can be equivalently expressed as $E = W/2$.

Once the cluster loses mass ΔM (so that its new mass is $M = M_0 - \Delta M$), the binding energy decreases. Because we have stipulated that the mass loss occurs over $< \tau_D$, we can assume that the radius and average stellar velocities of the system are unchanged. The energy of the system after mass loss is then

$$E = K + W = \frac{1}{2}\left[M \langle v_0^2 \rangle - \frac{GM^2}{R_0}\right]. \tag{1.4}$$

On a dynamical timescale, the system must expand to a new equilibrium radius R satisfying the virial theorem so that the new energy $E = W/2$. Using Equations 1.3 and 1.4, we find the radius to expand by a factor

$$\frac{R}{R_0} = \frac{M_0 - \Delta M}{2(M_0/2 - \Delta M)}. \tag{1.5}$$

We see that $R/R_0 \to \infty$ as $\Delta M \to M_0/2$, so the cluster will be completely disrupted if it loses half of its mass.

After initial gas expulsion and deaths of the cluster's most massive stars, stellar evolution continues to remove mass from the cluster, but slowly compared to τ_D. It is now appropriate to conserve the "adiabatic invariants" (the radial and azimuthal actions) of the stellar orbits within the cluster. As an example, in the outer halo of a cluster of mass M, the potential is roughly Keplerian, and the conserved actions can be written as:

$$J_2 = (GMa)^{1/2}(1 - e^2)^{1/2}; \quad J_3 = (GMa)^{1/2}[1 - (1 - e^2)^{1/2}], \tag{1.6}$$

where a and e are the semimajor axis and eccentricity of the stellar orbit within the cluster. Note that J_2 is just the specific angular momentum of a Keplerian orbit. $J_3 = J_r$, the radial action, is a closed loop integral of the radial momentum over the orbit, encompassing the extent of the radial oscillation between peri/apocenter; see B&T §3.5.2 for details.

Setting $J_2(M_0) = J_2(M_0 - \Delta M)$ and $J_3(M_0) = J_3(M_0 - \Delta M)$, we find that e must be constant and that $a \propto M_0/(M_0 - \Delta M)$. The shapes of the stellar orbits are conserved while the cluster expands so that

$$\frac{R}{R_0} = \frac{M_0}{M_0 - \Delta M}. \tag{1.7}$$

In this scenario, no physical amount of mass loss disrupts the cluster.

To summarize, impulsive mass loss ($\tau_{\text{mass loss}} \lesssim \tau_D$, caused by the deaths of and feedback/gas expulsion by massive stars) results in a greater degree of cluster expansion and is more destructive than adiabatic mass loss ($\tau_{\text{mass loss}} \gtrsim \tau_D$, caused by continued evolution of lower-mass stars). Clusters undergoing impulsive mass loss must lose relatively little mass (have high star formation efficiency) to remain bound. Lada et al. (1984) find exactly this behavior in N-body calculations that vary the modeled star formation efficiency and gas removal timescales. They also note that while clusters with instantaneous gas expulsion and star formation efficiencies <50% become globally unbound as in the Hills (1980) analytical prediction, a fraction of the stars are retained as a bound core. Baumgardt & Kroupa (2007) provide a more recent example of a set of larger N-body simulations exploring mass loss by gas expulsion. The same expected behavior can be seen in Figures 1.4 and 1.5, which show the retained fraction of bound stars and the expansion factor (R/R_0) as a function of star formation efficiency (the inverse of the fraction of mass lost), and of gas expulsion timescale.

If we ignore gas expulsion and consider a virialized cluster of formed and evolving stars, the number of massive stars formed plays an important role in cluster's evolution. Figure 1.6 shows the evolution of the bound mass and half mass radii of two nearly identically-initialized N-body simulations. Both consist of 15000 stars with an initial virial radius of 3 pc. The stellar masses are drawn from a Kroupa (2001) initial mass function, so that stochastic sampling results in significantly different mass contributions from high-mass stars (in this example, ∼1600 versus nearly 3000 $M_\odot$ of stellar mass come from stars $> 8M_\odot$). The cluster with more massive stars loses a higher fraction of its mass impulsively, expanding to ∼1.6 times the final size of the cluster with fewer massive stars (and later in the simulation, dissolving in only 40% of the dissolution time of the initially less massive cluster).

The variation in cluster dissolution speed due to mass loss from varied population sizes of OB stars can lead to drastically different resulting stream morphologies! See for example Wang & Jerabkova (2021).

1.3 Primordial binaries

Recommended Reading: Hurley et al. (2007); Offner et al. (2023)

As globular clusters are by definition very old, it is not possible to observe their primordial binary fractions. Present-day completeness-corrected radial velocity surveys of clusters like Omega Centauri, M4, NGC 3201, among others find binary fractions ranging from 2–20% (e.g., Wragg et al. 2024; Sommariva et al. 2009; Giesers et al. 2019; Milone et al. 2012). These

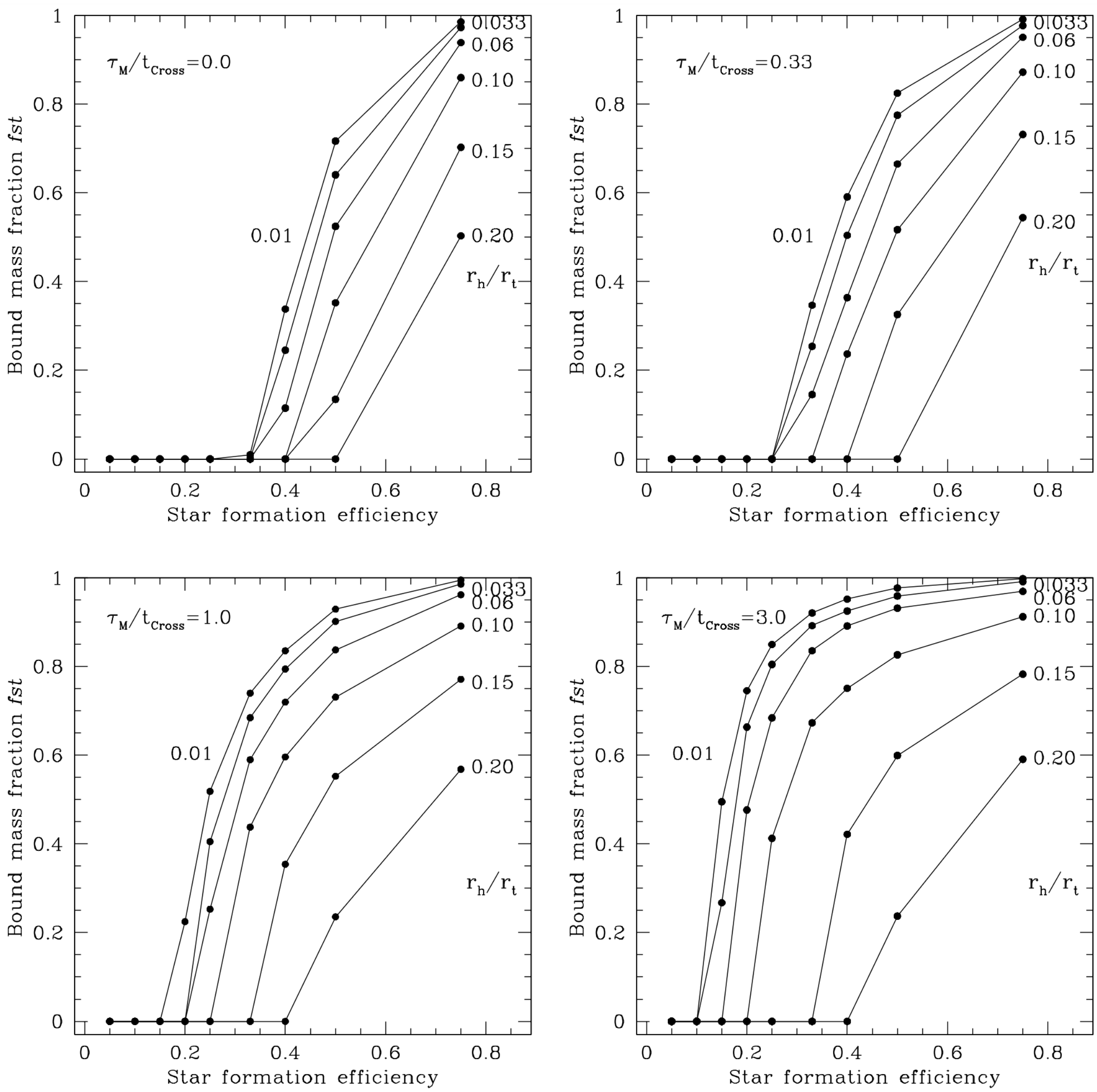

Figure 1.4: Figure 1 from Baumgardt & Kroupa (2007), showing the surviving fraction of bound mass as a function of star formation efficiency and gas expulsion timescale. The different curves on each panel correspond to different strengths of tidal field in which the clusters were evolved; higher r_h/r_t corresponds stronger influence from tides.

surveys are able to detect only the shorter-period binaries, before performing Monte Carlo experiments where an assumed underlying population of binaries is drawn and “observed” to determine the detection fraction (see as well the Via Science Book!). Unfortunately, it is nontrivial to convert from present-day binary fractions to primordial ones, since GC binaries undergo dynamical processing in the dense cluster environment. A discussion of hard and

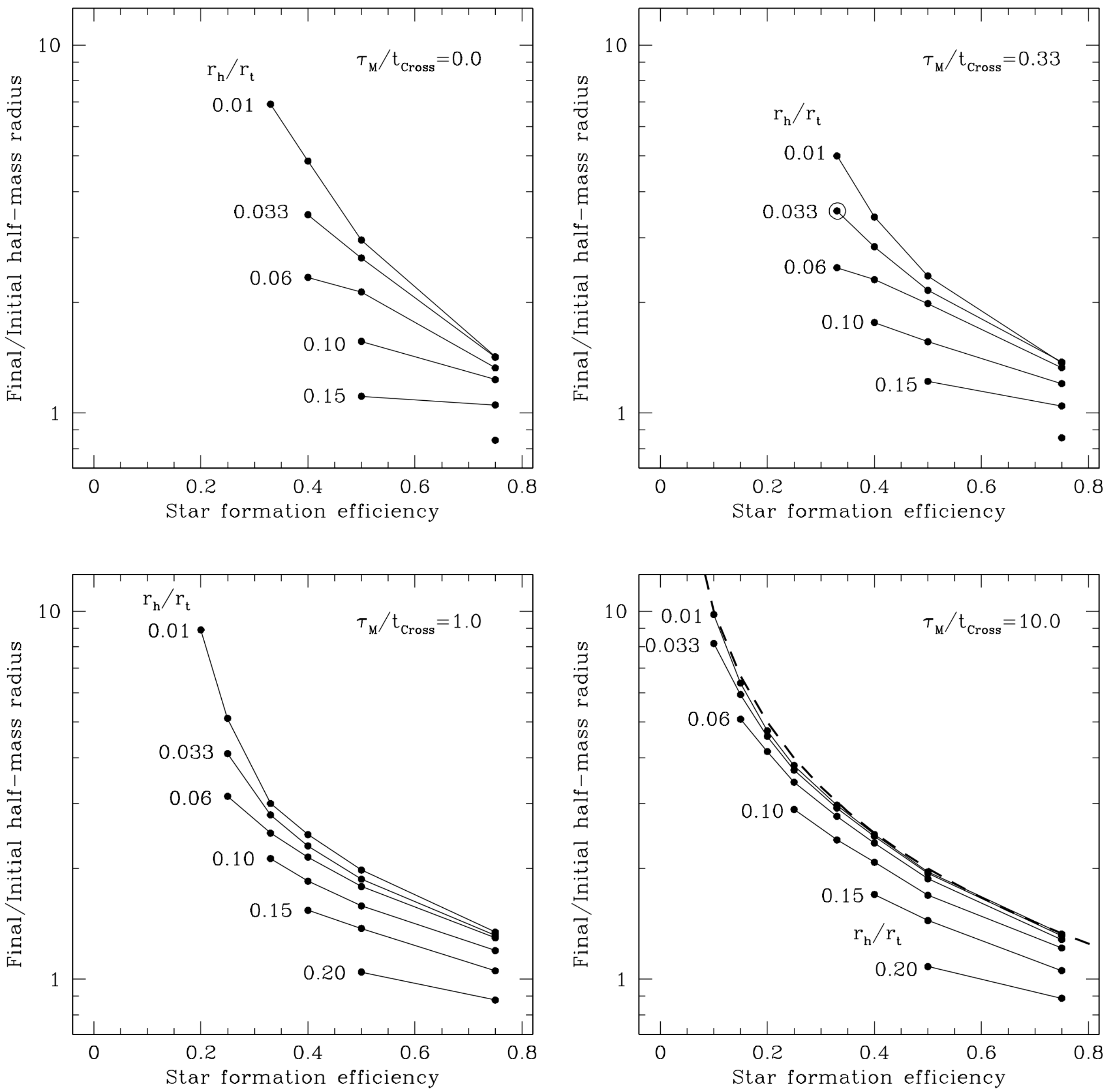

Figure 1.5: Figure 4 from Baumgardt & Kroupa (2007); same as Figure 1.4 but showing the cluster expansion factor (R/R_0).

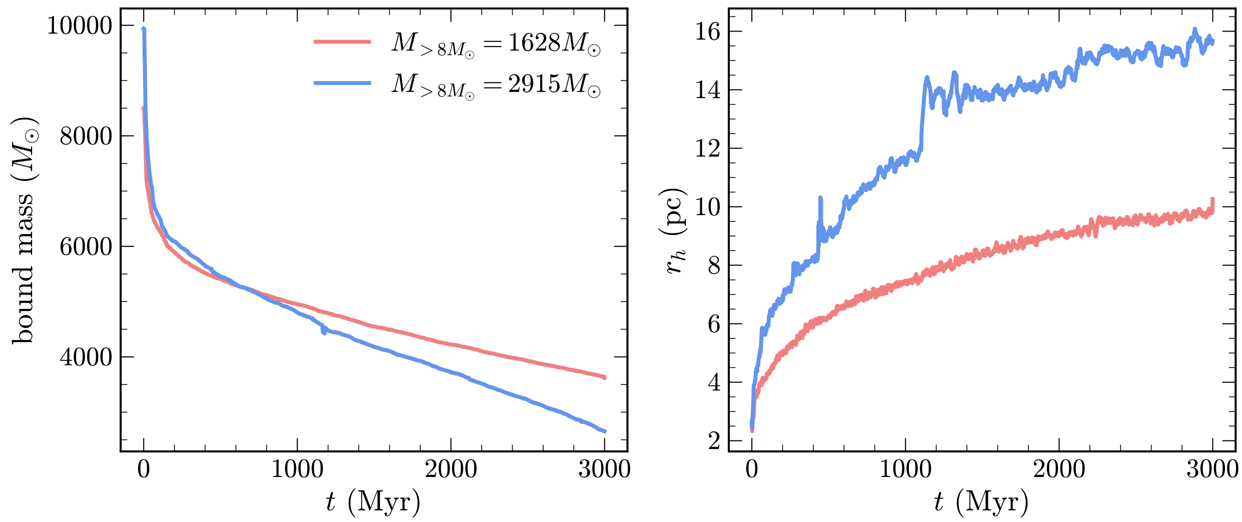

Figure 1.6: Unpublished N-body simulation data showing bound mass and half mass radius of two example N-body clusters over time.

soft binaries and their evolution in GCs is left for later.

It may be possible to glean insight into the primordial binary population in GCs through observations of young massive clusters, where we find completeness-corrected binary fractions of ~40–60% (e.g., Sana et al. 2013; Dunstall et al. 2015; Ritchie et al. 2022; Banyard et al. 2022), closer to that of field stars. Open clusters, such as those detailed in the *many* WIYN Open Cluster Survey (WOCS) papers (Mathieu, 2000), may also lend insight into the primordial binary fractions of clustered star formation. WOCS papers tend to report open cluster binary fractions between 20–50%. Comparisons between present-day open clusters or YMCs and ancient globular clusters should be drawn with caution, as binary demographics are strong functions of mass and metallicity, putting open clusters/YMCs in a very different regime from globular clusters (see more discussion below).

Simulation-based approaches to constraining GC initial binary populations reveal complex relationships between the primordial and present-day binary fractions. Hurley et al. (2007) initialize a suite of N-body simulations with binary fractions from 5–50% and find that low present-day binary fractions can be reproduced both by decreasing *and* increasing the primordial binary fraction. Ivanova et al. (2005) reproduce low present-day binary fractions in Monte-Carlo-based GC simulations with initial binary fractions as high as 100% (though, Fregeau et al. 2009 amend this claim and find results similar to Hurley et al. 2007 after updating their simulation algorithm).

It seems unlikely, though, that binary star formation in globular clusters is radically different

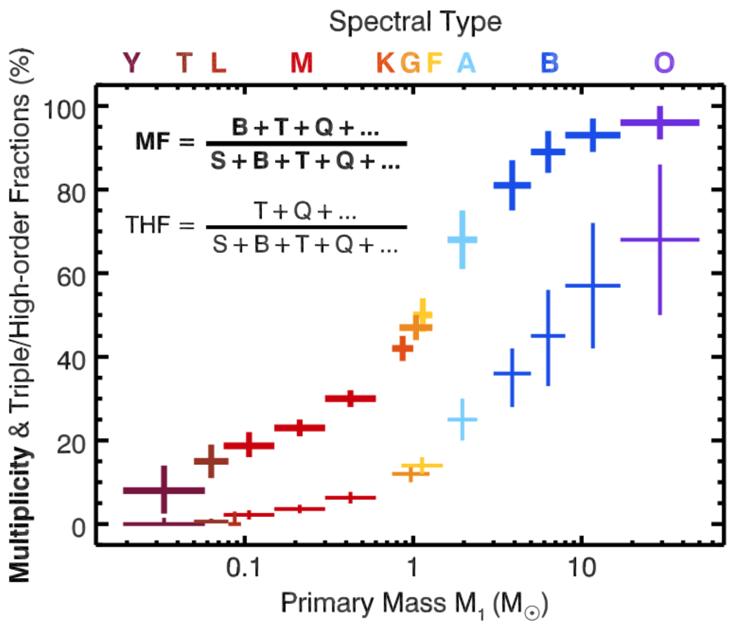

Figure 1.7: A portion of Figure 1 from Offner et al. (2023), showing the multiplicity frequencies as a function of primary mass.

from clustered star formation elsewhere, meaning that GC primordial binary demographics probably follow distributions similar to those prescribed for stars in other environments. Section 2 of Offner et al. (2023) provides a detailed overview of the current state of this field, but the main result of note is that binary fractions/multiplicity frequencies are strong functions of primary mass: M dwarfs have multiplicity frequencies of $\lesssim 10\%$, but this increases with mass so that O stars have multiplicity frequencies close to 100% (see Figure 1.7). Additionally, Moe et al. (2019) find a close binary fraction that strongly anti-correlated with metallicity, and show that the initial wide binary fraction should be independent of metallicity (the reason is that higher-metallicity star forming clouds have higher opacities, cool less efficiently, and fragment less). Hwang et al. (2022) find an increasing wide binary fraction with [Fe/H] in the present day thick disk and halo, but this is likely due to the fact that low-metallicity formation environments (such as globular clusters) have higher stellar densities that tend to disrupt initially-formed wide binaries. On the whole, we might expect similar wide-binary fractions to what are formed at present day in primordial GCs, whereas their primordial close-binary fractions may have been much higher than what we observe today.